Extreme Mechanics Letters 41 (2020) 101023

Contents lists available at ScienceDirect

Extreme Mechanics Letters

journal homepage: www.elsevier.com/locate/eml

Tandem actuation of legged locomotion and grasping manipulation in soft robots using magnetic fields

Venkatasubramanian Kalpathy Venkiteswaran [a,*], Danica Kristina Tan [a], Sarthak Misra [a,b]

[a] Surgical Robotics Laboratory, Department of Biomechanical Engineering, University of Twente, 7500 AE Enschede, The Netherlands
[b] Department of Biomedical Engineering, University of Groningen and University Medical Centre Groningen, 9713 GZ Groningen, The Netherlands

ARTICLE INFO

Article history:
Received 5 June 2020
Received in revised form 2 October 2020
Accepted 3 October 2020
Available online 10 October 2020

Keywords:
Soft robots
Biomimetic locomotion
Grasping manipulators
Magnetic actuation

ABSTRACT

Untethered soft robots have the potential to impact a variety of applications, particularly if they are capable of controllable locomotion and dexterous manipulation. Magnetic fields can provide human-safe, contactless actuation, opening the gates to applications in confined spaces — for example, in minimally invasive surgery. To translate these concepts into reality, soft robots are being developed with different capabilities, such as functional components to achieve motion and object manipulation. This paper investigates the tandem actuation of two separate functions (locomotion and grasping) through multi-legged soft robots with grippers, actuated by magnetic fields. The locomotion and grasping functions are activated separately by exploiting the difference in the response of the soft robots to the magnitude, frequency and direction of the actuating magnetic field. Two robots capable of performing controllable straight and turning motions are demonstrated: a millipede-inspired robot with legs moving in a rhythmic pattern, and a hexapod robot with six magnetic legs following an alternating tripod gait. Two types of grippers are developed: one inspired by prehensile tails and another similar to flowers or jellyfish. The various components are fabricated using a composite of silicone rubber with magnetic powder, and analyzed using quasi-static models and experimental results. Fully untethered locomotion of the robots and independent gripper actuation are illustrated through experiments. The maneuverability of the robots is proven through teleoperated steering experiments where the robots navigate through the workspace while avoiding obstacles. The ability of the robots to manipulate objects by operating in tandem with the grippers is demonstrated through multiple experiments, including pick-and-place tasks where the robots grasp and release cargo at specific locations when triggered using magnetic fields.

1. Introduction

In recent years, the field of soft robots has garnered significant interest, spurred on by the utilization of soft materials to create flexible, adaptable structures with resilience to large deformation [1–3]. Soft robots have the ability to conform to their surroundings, reducing the risk of damage from impact and simplifying grasping actions [4,5]. Many soft robot designs are inspired by highly functional and compliant biological components (such as elephant trunks, fish bodies, reptile flippers and gecko feet), and biomimicry is often used to create flexible, functional and resilient robots [6,7]. Recent work aimed at medical applications has focused on creating robotic devices made entirely of soft and biocompatible materials [8–11].

Magnetic actuation represents an untethered form of energy transfer, particularly suited to miniaturized robots from millimeter to nanometer scales [12–14]. The actuation response is instantaneous and magnetic fields are compatible with many media, including vacuum and fluids (electrically conducting and non-conducting). Soft robots controlled by magnetic fields (or 'magnetic soft robots') are fabricated with magnetic-polymer composites (MPC) and actuated using external magnetic sources (electromagnets or permanent magnets), eliminating the need for an on-board power supply and allowing the robot to function as long as the external source is active [15]. Miniaturized designs capable of complex motion are made possible through the use of design-specific magnetization profiles [16–18]. For instance, flexible magnetic robots fabricated from a single strip of MPC have successfully demonstrated swimming motion, flagella-based propulsion, rolling, jumping and other methods of locomotion [19–21]. Magnetic soft robots are particularly suited to medical applications because magnetic fields are not harmful to humans, and these robots can potentially be imaged and controlled

* Corresponding author.
E-mail address: v.kalpathyvenkiteswaran@utwente.nl (V.K. Venkiteswaran).

https://doi.org/10.1016/j.eml.2020.101023
2352-4316/

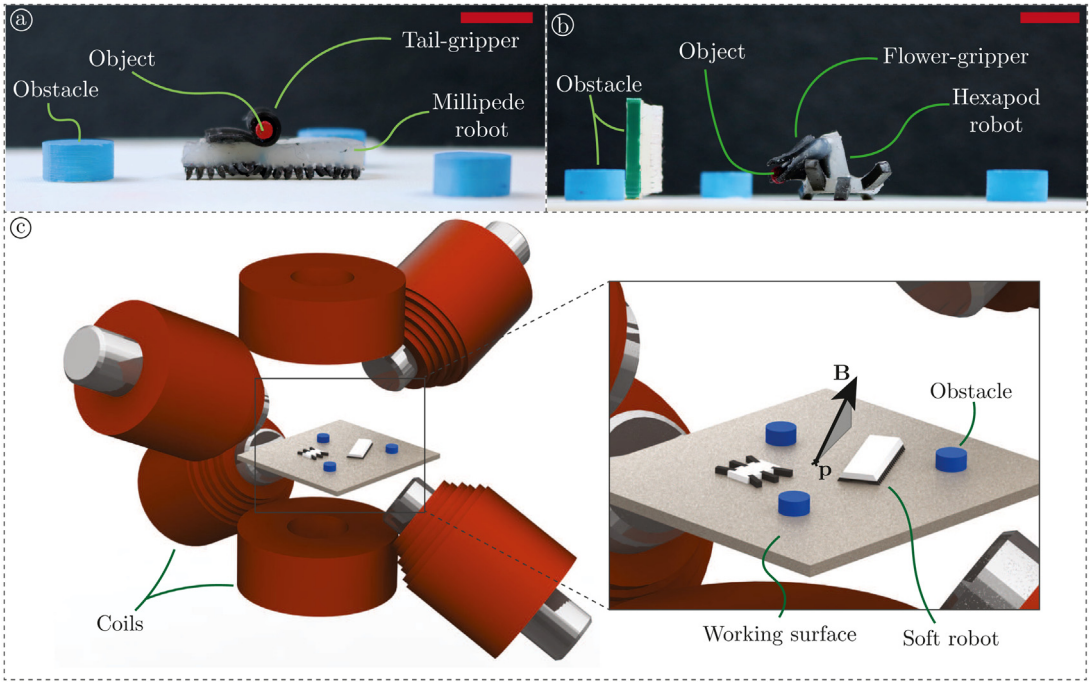

Fig. 1. Small-scale magnetic soft robots capable of tandem actuation of grasping and locomotion. ⓐ 'Millipede robot' with a 'Tail gripper' carrying a cylindrical object and ⓑ 'Hexapod robot' with 'Flower gripper' carrying a spherical object. Scale bar is 10 mm. ⓒ The actuation of the soft robots is achieved using BigMag: an array of six movable electromagnetic coils, capable of generating a magnetic field (**B**) at any point (**p**) within the workspace.

using clinically-relevant techniques such as magnetic resonance imaging (MRI) [22–24]. Recent developments have focused on improving fabrication techniques for magnetic soft robots to produce a variety of shape changes and deformation modes [25–27]. Untethered micro-scale grippers actuated using magnetic fields have been developed by many groups while also incorporating responses to other stimuli (heat, light, chemical reagents) [28–32]. Manipulation of target objects in 3D in a liquid medium have been demonstrated using untethered grippers actuated through a combination of magnetic forces and magnetic torques [33,34]. Other work has demonstrated magnetically-actuated soft robots capable of motion and grasping on solid substrates where the two functions use coupled actuation modes which restrict the robots to locomotion through rolling motion [20,25,27]. By contrast, this work investigates an alternate approach to decouple two separate actions (in this case, legged locomotion and grasping) in a magnetically-actuated soft robot while demonstrating maneuverable locomotion across a solid surface.

In this paper, the design of bio-inspired multi-legged soft robots with grasping manipulators (Fig. 1) is described. The locomotion of the soft robots and the actuation of the grippers are achieved in a fully untethered manner using external electromagnets. The robots and grippers are designed and paired such that the locomotion and grasping functions can be independently actuated using magnetic torques, in contrast to other works in literature. This is achieved by exploiting the difference in actuation response between the robot legs and the grippers by controlling the magnitude, frequency and orientation of the actuating magnetic field. The robots and grippers are made using MPC and magnetized in specific patterns to realize actuation modes that are complementary to one another. Maneuverable locomotion of the robots is achieved using multiple legs that generate variable displacement, which is achieved through geometric biasing of magnetic dipoles within the robot body. The robots are demonstrated to have repeatable locomotion characteristics, including reliable accuracy of steering. The grippers grasp and release objects when triggered, and hold on to the object during the locomotion of the robot. The robots and grippers are engineered such that the locomotion and grasping function do not interfere with one another. The tandem functioning of the robots and grippers is demonstrated through experiments where they maneuver around obstacles and perform pick-and-place tasks.

The primary contributions of this work are:

- Independent operation of two functional elements (legs and grippers) on a soft robot, and utilization of the variable actuation response from changing the magnitude, frequency and orientation of the external magnetic field.
- Design of the soft robots capable of controllable steering and maneuverability through magnetic and mechanical biasing.
- Development of magnetic grippers that can open and close using magnetic fields that do not adversely affect the motion of the robots.

Additionally, the paper demonstrates all of these contributions through multiple experiments while navigating the workspace through teleoperated control.

2. Materials and methods

2.1. Magnetic actuation

The actuation of the soft robots in this work is achieved using magnetic fields. The robots are produced with functional magnetic elements (legs for locomotion, grippers for grasping). The magnetic dipoles in the robot are controlled by the fabrication process. The interaction of an actuating magnetic field with the magnetic dipole moments inside the soft robot leads to mechanical loads (magnetic torques) that deform the soft material (Sec. S.1). The locomotion gait patterns and grasping action are produced by controlling the amplitude and direction of the actuating magnetic field. The actuation of the individual soft robots and grippers is described in detail in Section 3.

In this work, the actuating magnetic fields are generated using a moving array of six electromagnetic coils in which the coils

rotate around a spherical workspace of diameter 10 [cm], enabling the system to produce magnetic fields up to 60 [mT] with a bandwidth of 40 [Hz] (BigMag [35]). Two cameras are used for observing the top and side views of the experiments.

2.2. Soft robots and grippers

The soft robots and grippers are engineered to respond to actuation such that their functions can be independently activated by varying the magnitude, frequency and orientation of the external magnetic field. Additionally, the robots are designed such that they can be steered by generating variable displacements on either side of the robot body.

Two types of soft robots and two types of grippers are presented in this paper. All four are shown with their dimensions and fabrication process in Fig. 2. The first robot is inspired by myriapods such as millipedes and centipedes, and named Millipede robot. In nature, these organisms achieve locomotion by utilizing Central Pattern Generators (CPGs) to coordinate limb function in groups [36]. The legs of the robot are activated in a sequential metachronal rhythm, with a noticeable wave-like characteristic. Other works in literature have developed myriapod-inspired robots, although the focus was on achieving motion of individual legs [37,38]. In previous work, we demonstrated the use of metachronal rhythm to generate effective soft robot locomotion capable of traversing uneven terrain while maintaining a low, stable profile [39]. In this work, the robot is designed with two sets of legs and a longitudinally symmetric tilt in magnetic dipoles to make the Millipede robot steerable (Fig. 2ⓐ–ⓓ).

The other soft robot described in this paper is a six-legged robot, named Hexapod (Fig. 2ⓔ–ⓗ). It has an alternating tripod gait inspired by ants and other arthropods, with three pairs of legs [40,41]. Each pair of legs is anti-symmetric, that is, one leg is out of phase with the other. This leads to three of the legs making contact with the ground at any point during the gait cycle, forming a tripod support. The other three legs make contact with the ground during the opposite half-phase of the gait cycle.

In order to grant functional properties to the robots, two bio-inspired gripper designs are also produced. The Tail gripper developed here is inspired by prehensile tails (seen in organisms such as new world monkeys, seahorses, and pangolins) and consists of a flat piece of magnetic silicone which can be attached to the robot (Fig. 2ⓘ–ⓚ). The Tail utilizes a rolling action to wrap around an object. So as to not interfere with the locomotion mode of the robot, the Tail is designed such that the minimum magnetic field needed to actuate it is higher than that required for locomotion of the robot. This allows the robot to move without activating the gripper. Additionally, the Tail stays coiled after actuation, eliminating the need continuously activate the gripper after the grasping action is complete.

Inspiration for the second gripper design – the Flower gripper (Fig. 2ⓛ–ⓝ) – comes from various flowering plants and organisms such as jellyfish, tapeworms and carnivorous plants like bladderworts. Two variations are produced — a 3-petal version and a 4-petal one. Both designs are in the shape of hollow pyramids where a target object may be held. The bottom half of the edges of the pyramids are sealed with silicone, leaving the grippers open at the apex. In its unactuated state, the gripper's opening is held partially shut by the shape of the petals, and the gripper resembles a pyramid. The petals can be opened and closed using an external magnetic field to perform the grasping action.

2.3. Fabrication

In this work, all the magnetic components are made from a magnetic polymer composite (MPC). The MPC comprises a silicone rubber matrix (Ecoflex-0010, Smooth-On Inc., USA) and a ferromagnetic powder of PrFeB with a mean particle size of 5 [μm] (MQFP-16-7-11277, Magnequench GmbH, Germany). The mass ratio of the magnetic particles to the silicone rubber in the MPC is defined by the magnetic mass fraction (R). The non-magnetic components are made from the silicone rubber without any magnetic particles. For the robots, the legs are made from MPC while the body is non-magnetic, while the grippers are made entirely from MPC.

The robots and grippers are produced using an iterative molding and curing process. Molds are created using 3D printed plastic or laser-cut acrylic to create the shapes for the soft robotic components. The MPC is set to cure in the molds at room temperature (24 [°C]) for four hours and then subjected to a 1 [T] magnetic field using an electromagnet (B–E 25 electromagnet, Bruker Corp., USA). The magnetization process orients the dipoles in the MPC to design-specific directions. During this step of the fabrication process, the components are constrained using fixtures to ensure the alignment of magnetic dipoles within the material will produce the desired actuation response.

Fig. 2 demonstrates the steps in the fabrication process of the robots and the grippers. For the Millipedes, each set of magnetic legs ($R = 2{:}1$) is made individually, with a layer of silicone rubber at the top, and magnetized using custom-made helical fixtures to achieve a sinusoidal magnetization profile. Two sets of legs are then set in a mold such that the plane of the magnetic dipole moments in each set of legs is tilted by an angle ($\phi = 30°$) from the vertical plane, and more silicone rubber is used to join the legs, forming the body.

For the Hexapods, the magnetic legs ($R = 3{:}2$) are made as individual components and magnetized in circular arcs of 90°. Three of the legs are magnetized with the tips aligned towards the north pole of the electromagnet while the other three have their tips aligned to the south. The legs are then placed in molds and silicone rubber is added to create the body.

The grippers are made entirely of the MPC. The Tail grippers are made as rectangular strips of desired dimensions using 3D printed molds. For magnetization, the Tails are wrapped and secured in the form of a spiral around a wooden dowel of 2.45 [mm] diameter, which produces an undulating magnetization profile when unwrapped.

For the origami-inspired Flower gripper, a flat shape is first produced with the MPC ($R = 1{:}4$), and magnetized such that the dipole moments are all oriented normal to the surface of the gripper. It is then wrapped around a pyramidal wax form and silicone rubber is applied as an adhesive to form the final shape. Once set, a heat gun is used to melt the wax within the manipulator while ensuring the temperature remains well below the Curie temperature of the material (345 [°C]). The resultant shape is a pyramid that is closed on one end and open on the other.

The choice of the magnetic mass fraction (R) is dependent on the actuation and fabrication process. For the robots in this paper, we aim to maximize (R) in order to achieve actuation using lower magnetic fields. In the case of the Millipede, ($R > 2$) leads to air pockets and clumping of magnetic powder in the legs, while for the Hexapod, ($R > 1.5$) results in strong magnetic moments in the legs resulting in magnetic adhesion between adjacent legs. For the grippers, lower values ($R < 1$) are used to ensure actuation occurs at higher magnetic fields to separate their actuation from the locomotion of the robots. Both grippers are made from thin strips of MPC, and lower values of (R) help prevent air pockets and clumping of magnetic powder during fabrication.

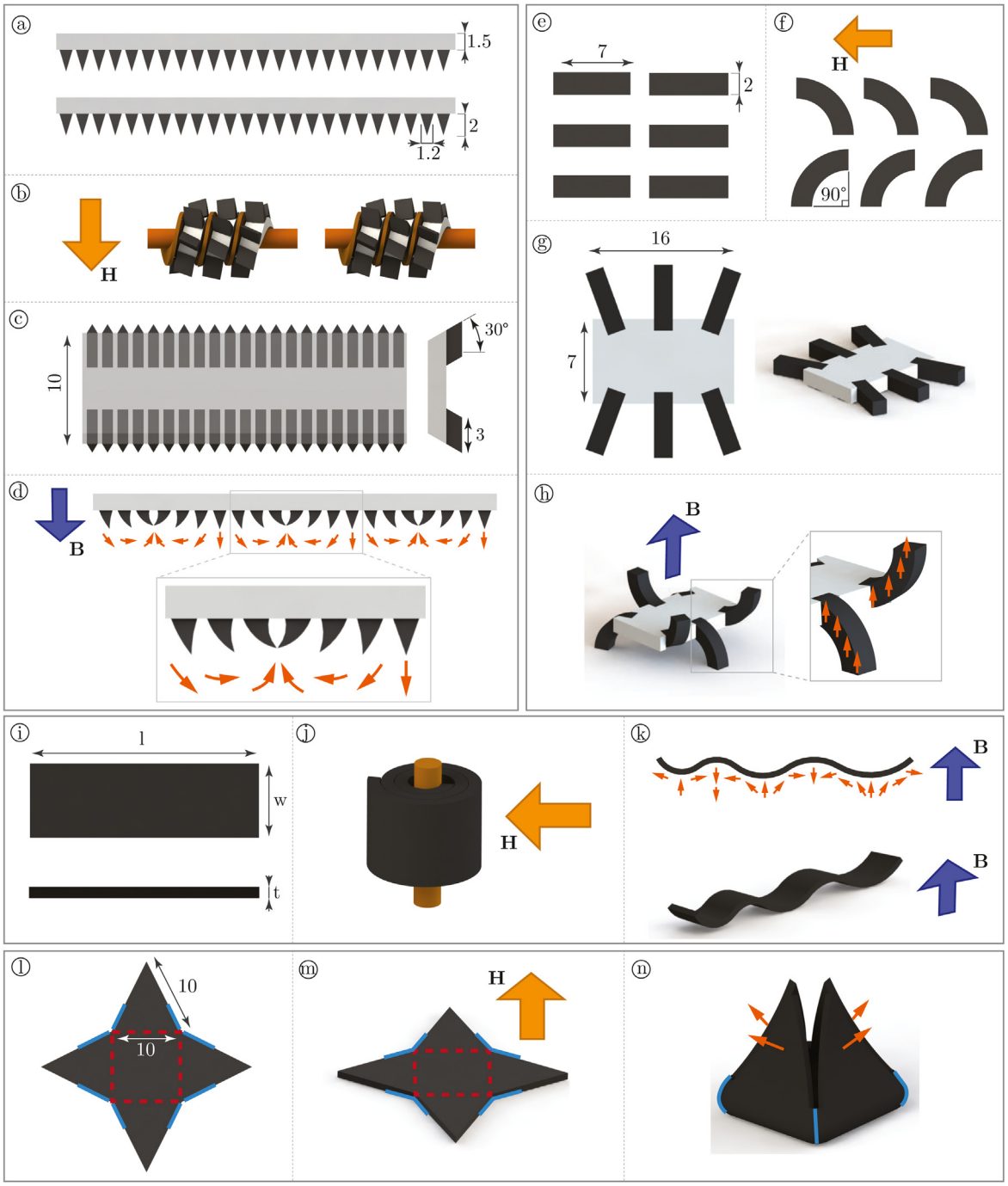

Fig. 2. The soft robots are fabricated using a combination of silicone rubber (white) and magnetic polymer composite (black). ⓐ The Millipede robots have two sets of legs, which are fabricated separately and ⓑ subjected to a magnetization field (**H**) while constrained using helical fixtures in order to obtain a sinusoidal magnetization profile. ⓒ The two sets of legs are joined together to form the robot (top and front view are shown). ⓓ Under an external field (**B**), the legs deform to align their magnetic dipoles (orange arrows) with the field, while the non-magnetic body remains undeformed. ⓔ–ⓕ For the Hexapod robots, the six legs are fabricated individually and magnetized in a quarter-circle shape (with tips of three legs pointing in the direction of the field and other three in the opposite direction as shown). ⓖ The legs are assembled into the non-magnetic body. ⓗ Under an external field, three legs lift the robot off the floor while the other three remain off the ground. ⓘ The tail-like grippers are fabricated as flat strips (dimensions l, w, t) and ⓙ magnetized while wrapped around a rod to form a spiral shape. ⓚ This produces an undulating shape when a magnetic field is applied, with the magnetic dipoles (orange arrows) trying to align themselves to the external magnetic field. ⓛ–ⓝ The Flower grippers are fabricated and magnetized in a flat shape (design with four petals is shown). After magnetization, the petals are folded along the dashed lines and silicone rubber is applied along the marked edges to join adjacent petals at the base, generating the final pyramidal shapes with the magnetic dipoles perpendicular to the faces of the pyramid. Dimensions are marked in [mm]. (For interpretation of the references to color in this figure legend, the reader is referred to the web version of this article.)

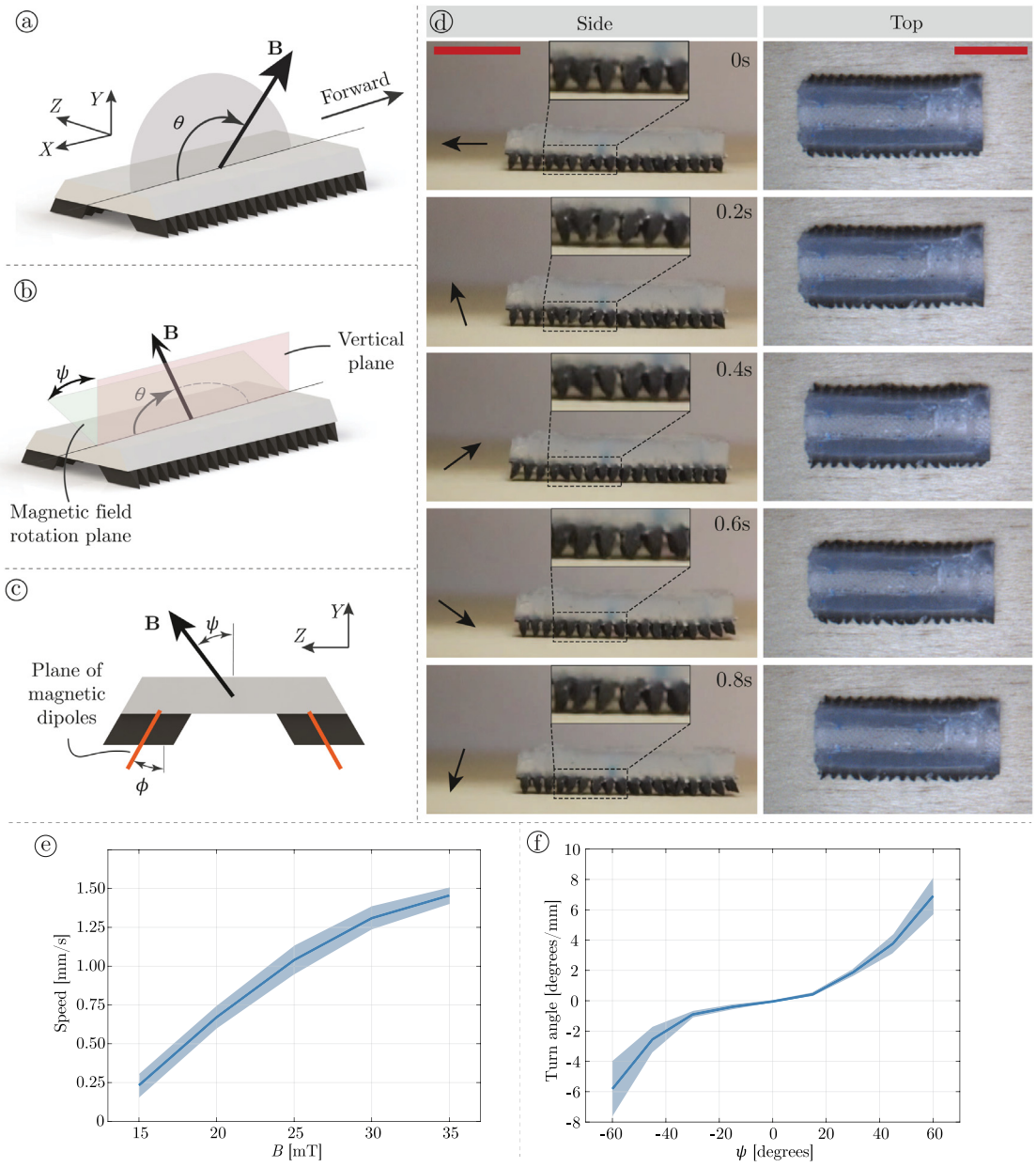

Fig. 3. The Millipede robots are actuated using rotating magnetic fields. ⓐ For straight-line locomotion, the magnetic field (**B**) of constant magnitude is rotated ($\theta \in [0°, 360°]$) in the vertical plane (XY). ⓑ For turning locomotion, the magnetic field is rotated in a plane tilted by an angle (ψ) from the vertical. ⓒ Back view illustrating direction of magnetic dipoles in legs (aligned at angle $\phi = 30°$ to the vertical) and direction of magnetic field vector. ⓓ Images of Millipede robot during straight-line locomotion over one gait cycle, with the experiment time and direction of the magnetic field (25 [mT]) also shown. Magnified images of six legs of the Millipede are shown in the insets. Scale bar is 10 [mm]. ⓔ Speed of the millipede robots as a function of the magnitude of the actuating magnetic field (B). The time period of rotation of the magnetic field is $T = 1$ s. ⓕ The change in heading of the millipede robots as a function of the tilt angle (ψ). Positive and negative angles indicate right and left turns, respectively. Mean values across three specimens are shown, with the shaded region representing standard deviation.

3. Results

In this section, the experiments demonstrating the magnetic actuation of the soft robots and grippers are presented. The actuation techniques necessary for the locomotion of the robots are described, along with influence of the designs and magnetization profiles on the results. The locomotion characteristics (speed and maneuverability) are tested. Following this, the actuation of the grippers in order to achieve the grasping function is described. For each component, the mechanical response of the soft robotic elements to the magnetic field is analyzed using theory and experiments, and inferences are drawn from the results (Sec. S.2). After the results of the individual components, the working of the robots and grippers in tandem is demonstrated using teleoperated steering and pick-and-place tasks.

3.1. Millipede

The Millipede soft robot presented here has two sets of legs, magnetized and attached (to a non-magnetic body) such that each set of legs has dipoles aligned in a plane tilted at an angle ($\phi = 30°$) from the vertical plane. The magnetic dipoles in each set of legs follow a sinusoidal profile, enabling the robot to move under rotating magnetic fields [39].

Fig. 3ⓐ–ⓒ illustrates the concept. Fig. 3ⓓ shows the robot during motion, where it is noticeable that the legs do not make contact with the substrate during all phases of a motion cycle

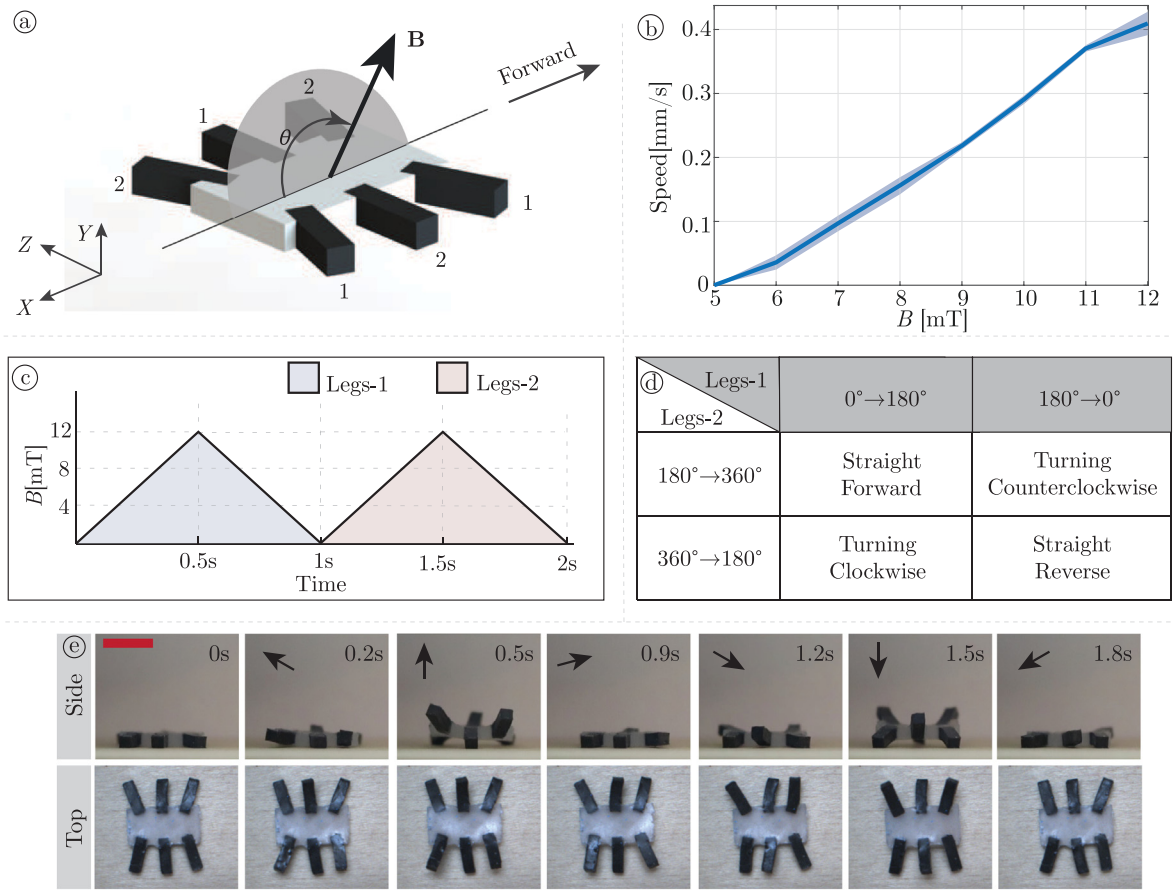

Fig. 4. ⓐ The locomotion of the Hexapod robot is achieved through actuation of each set of legs (labeled 1 and 2) in separate cycles. The magnetic field (**B**) rotates in the vertical plane (XY) by the angle (θ) measured from the X-axis. ⓑ Plot showing the variation of speed of Hexapod robots as a function of the magnitude of the maximum magnetic field (B) used for actuation. Mean values across three specimens are shown, with the shaded region representing standard deviation. ⓒ The magnitude of the magnetic field (B) ramps up and down during each cycle of time period 1 [s], activating Legs-1 in one cycle and Legs-2 in the next cycle. ⓓ Maneuvering the robot requires changing the limits of θ for each actuation cycle, with the values for Legs-1 and Legs-2 tabulated (in degrees). Clockwise is defined as viewed from the top (XZ plane). ⓔ Images of the robot during forward locomotion, with the experiment time and direction of magnetic field shown. Scale bar is 10 [mm].

(Video SV1). Since the magnetic dipoles in the two sets of legs are symmetric about the vertical plane (XY), a rotating magnetic field (**B**) in this plane produces straight-line locomotion. By tilting the plane of rotation of the magnetic field by an angle (ψ), each set of legs experiences a distinct magnetic torque, producing greater displacement on one side of the robot compared to the other. This difference in displacement is used to generate turning motion that can be controlled using the tilt angle (ψ).

The magnitude of the magnetic field influences the speed of motion of the Millipede robot. It is observed that the legs achieve displacement due to each leg following a different trajectory during the return stroke compared to the forward stroke during the gait cycle (Sec. S.2.1). Increasing the magnetic field increases the disparity between the forward and return strokes, generating greater displacement. This is illustrated in Fig. 3ⓔ, where the speed of the robots increases with the magnetic field. While the magnetization in the form of a helix does create a helical angle in the direction of magnetic dipoles in the legs, the symmetry across the two sets of legs negates that effect and leads to straight-line motion.

Another important aspect and contribution of the design presented here is the ability to control the heading of the robot. This is tested by varying the tilt angle (ψ), and the results are shown in Fig. 3ⓕ (Video SV1). The data shows that varying the tilt angle produces a predictable change in the heading of the robot. When (ψ = 0°), the robots move ahead in a straight line, whereas a positive value of (ψ) makes the robot turn to its right and a negative value makes the robot turn left. This allows us to control the heading of the robot using a single control input (ψ). For both experiments, the robots show good repeatability (measured across three specimens) as evidenced by the standard deviations shown in the graphs.

3.2. Hexapod

The Hexapod soft robot is inspired by the alternating tripod gait locomotion of six-legged arthropods. As illustrated in Fig. 2, it has six magnetic legs and a non-magnetic body, with three of the legs magnetized with the dipoles at the tips oriented towards the magnetic north, while the others are magnetized with the tips oriented towards the magnetic south. The legs are assembled onto the robot body in an alternating manner (Fig. 4ⓐ). Locomotion of the robot is achieved by applying a magnetic field (**B**) on a vertical plane along the length of the robot (XY) and rotating the magnetic field vector about the lateral axis (Z). The direction of **B** is defined by the angle (θ) it makes with the horizontal plane (XZ). When a magnetic field is applied directed towards $+Y$ ($\theta = 90°$), only three legs (those with tips directed towards the magnetic south) make contact with the ground, while the other three are lifted into the air. Therefore, by rotating the field through the upper half-plane ($\theta \in [0°, 180°]$), the robot is displaced forward, but biased towards the side which has only

one leg making contact with the ground (Fig. 4ⓔ). Conversely, rotating the field through the lower half-plane produces locomotion with the other legs, biased to the opposite side. Alternating the magnetic field rotation between the upper and lower half-planes produces straight-line locomotion, and other combinations generate turning locomotion (Fig. 4ⓒ–ⓓ, Video SV1).

The motion of the Hexapod robots is also influenced by the magnitude of the magnetic field. At higher fields, the legs experience greater magnetic torques, therefore generating more displacement in the horizontal and vertical directions and also lifting the body further from the ground. This produces greater displacement during each gait cycle (Sec. S.2.2). Fig. 4ⓑ shows the speed of the robots using the alternating actuation pattern described above is presented in Fig. 4ⓒ–ⓓ. As the magnetic field increases, the legs displace more and lift the body further off the ground, producing greater displacement. However, there are limits to the relationship between the magnitude of the magnetic field and the displacement of the Hexapod. At higher fields, the legs lift the robot body too high from the substrate, causing unstable motion. For the experiments in Fig. 4ⓑ , the observed motion is unstable above 12 [mT].

3.3. Tail gripper

The Tail gripper is capable of wrapping around a target object and remaining rolled after the actuating magnetic field is removed (Fig. 5, Video SV2). The Tail only rolls when the magnitude of the magnetic field is above a threshold, which we denote by the magnetic field threshold (B_{min}). Additionally, the Tail gripper only functions when the field is rotated at a lower frequency ($<$0.1 [Hz]) than what is generally used for the locomotion of the robots (1 [Hz]). At higher frequencies, the tip of the Tail flaps back and forth in an oscillatory motion, rather than achieving the rolling action (See Section 3.5). The rolling action of the Tail performs better when it starts from the end which is attached to the dowel (i.e. has smaller radius of curvature) during magnetization (Fig. 2). It is also capable of rolling action if constrained from a height without the support of the substrate below (Video SV2).

In order to achieve the rolled shape, the magnetic actuation must overcome gravity and elastic energy in the Tail. An energy-based approach is used to obtain theoretical predication for B_{min}. The model is validated by producing tails of varying thicknesses, widths, and material ratios and experimentally determining B_{min} (Sec. S.2.3). From the results, we infer that the two main factors that affect B_{min} are the magnet to polymer mass ratio (R) and the thickness of the Tail. Knowing the value of B_{min} allows us to choose a Tail that is suitable for pairing with a particular robot.

3.4. Flower gripper

The Flower gripper is produced in the shape of a pyramid, which opens when a magnetic field is applied pointing towards the base of the gripper, and closes when the magnetic field is towards the apex of the pyramid (Fig. 6, Video SV2). The magnitude of the magnetic field controls the width of the opening. In the non-activated state, the gripper is in its closed form, enabling it to hold grasped objects without the need for an actuating magnetic field. Unlike the Tail gripper, there is no minimum field required to activate the Flower gripper. However, it opens and closes only under the influence of magnetic fields in its axial direction. This property is used to separate the function of the gripper from the motion of the robot as explained in Section 3.5.

The maximum grasping force generated by the gripper is determined experimentally (Sec. S.2.4). The 3-petal design produced a force of 15.6 $\pm$ 0.8 [mN], while the 4-petal version recorded a force of 23.5 $\pm$ 3.3 [mN], each over three repetitions.

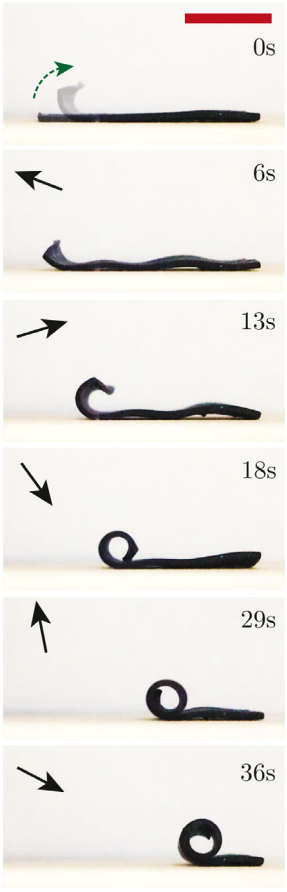

Fig. 5. ⓐ Demonstration of actuation of the single Tail gripper using a magnetic field (B = 15 [mT]) rotating at low frequency (0.05 [Hz]). The direction of the magnetic field and time of the experiment are shown. The gripper is not attached to the substrate. Scale bar is 10 [mm].

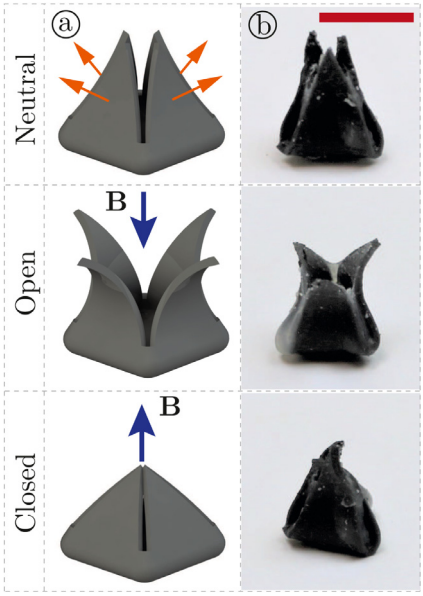

Fig. 6. ⓐ Schematic of 4-petal Flower gripper. The gripper after fabrication is in the form of a pyramid with the magnetic dipoles (orange arrows) in each petal aligned perpendicular to the surface. The gripper can open or close upon the application of a magnetic field (**B**) along the axis of the pyramid, depending on the magnitude and direction of **B**. ⓑ Images of 3-petal design. Scale bar is 10 [mm]. (For interpretation of the references to color in this figure legend, the reader is referred to the web version of this article.)

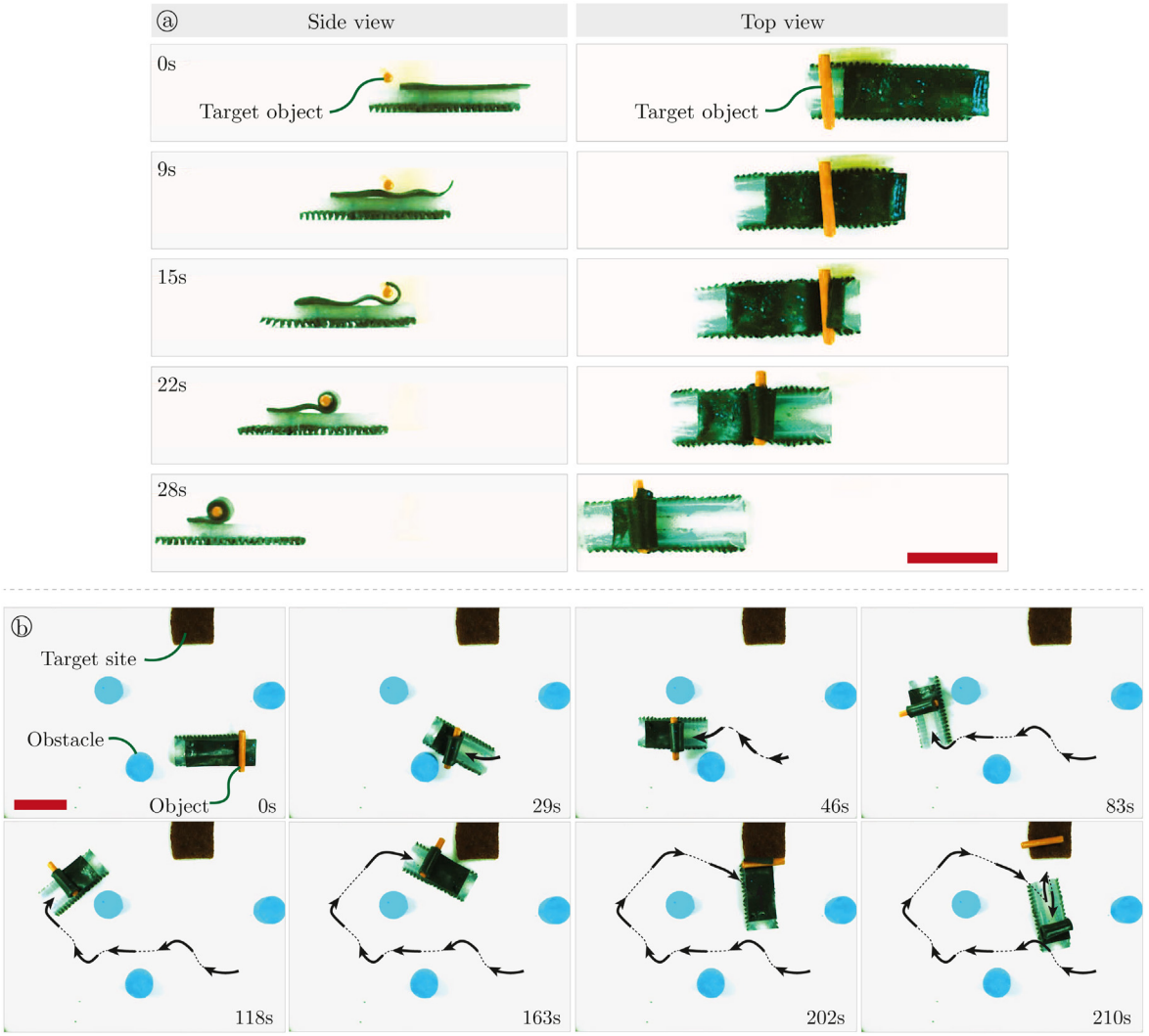

Fig. 7. ⓐ Experiment demonstrating Millipede robot with Tail gripper grasping an object from the workspace. The object is attached to a wall (not shown). The robot approaches the object with the Tail remaining unfurled using a fast-rotating magnetic field (25 [mT] at 1 [Hz]), after which the Tail is activated using a higher magnetic field which rotates more slowly (40 [mT] at 0.1 [Hz]) in order to grab the object. ⓑ Experiment showing Millipede robot with Tail gripper performing a pick-and-place task. The robot first gathers the object, then navigates past obstacles to reach a target site, and deposits the object by unfurling the gripper. Scale bar is 20 [mm].

3.5. Demonstrations of tandem actuation

The robots and the grippers are paired such that their actuation modes are complementary to one another, as described below. The Millipede robots are paired with the Tail grippers since they are both actuated using rotating magnetic fields. The Tail grippers require higher magnetic fields rotating at a lower frequency compared to the fields required for the actuation of the Millipede robots. The Flower grippers are attached to the Hexapod robots in a configuration which ensures that the axial direction of the gripper is along the length of the robot. Therefore, the direction of magnetic field required for actuation of the gripper is orthogonal to the magnetic field required for actuation of the legs of the robot. This pairing ensures that the robots and grippers can function independently. The grippers are attached to the robots using silicone rubber (Ecoflex 00-35 FAST, Smooth On Inc., USA).

Experiments are conducted to demonstrate the maneuverability of the robots, the function of the grippers and their combined actuation. The maneuverability of the robots is demonstrated by guiding them to a target location within the workspace while avoiding obstacles. The grasping functionality is illustrated through tasks where the robots either pick up objects from the environment or place them at target locations. The different modes of actuation are programmed into the system and controlled through teleoperation. Camera images are used by the operator to determine the position and orientation of the robots within the workspace.

Image sequences from the experiments with the Millipede robots and Tail grippers are presented in Fig. 7. In the first experiment (Fig. 7ⓐ, Video SV3), the Millipede robot walks towards the target object (a wooden rod), slows down and activates the gripper to grab the object, and then continues to move forward while grasping the object. The gripper remains unfurled while the robot moves towards the target, and remains rolled while the robot moves away, demonstrating the independent actuation of the robot and the gripper. The Tail is also able to dislodge the rod from the environment while grasping. It is worth noting that the Tail does not roll onto itself until the frequency of rotation of the magnetic field is reduced and the magnetic field is increased, until which point the tip oscillates up and down. In the second experiment (Fig. 7ⓑ, Video SV3), the robot captures an object by activation of the Tail gripper, traverses the workspace while avoiding obstacles to reach a target location, and

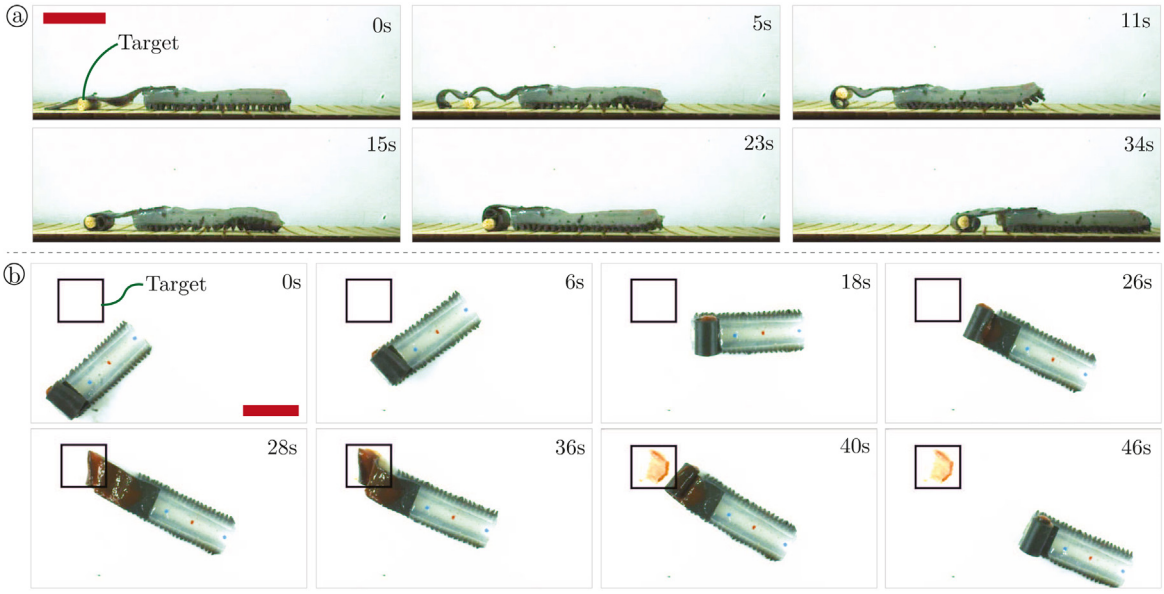

Fig. 8. ⓐ Experiment demonstrating Millipede robot with Tail gripper grasping an object from the substrate. The target object is positioned below the Tail, which is actuated to roll and grasp using a slow-rotating magnetic field (40 [mT] at 0.1 [Hz]). After the object is secured, the robot moves away (25 [mT] at 1 [Hz]). ⓑ Experiment illustrating Millipede robot with Tail gripper performing secure transport and delivery of a substance (orange dye mixed into water-soluble gel) to a target location. The robot first navigates to the target site (25 [mT] at 1 [Hz]) while ensuring the substance remains within the Tail. The Tail is then unfurled (30 [mT] at 0.1 [Hz]) to transfer the substance onto the substrate. Following this, the Millipede secures the Tail and moves to away from the target site (25 [mT] at 1 [Hz]) with only the target area stained by the substance. Scale bar is 20 [mm]. (For interpretation of the references to color in this figure legend, the reader is referred to the web version of this article.)

deposits the object by unfurling the gripper. This demonstrates the maneuverability of the robot, the ability to keep the gripper activated during locomotion, and reversed actuation of the gripper to release the object at the target site. It is worth noting that during the activation of the Tail gripper, the Millipede robot does undergo displacement due to the influence of the rotating magnetic field. However, this displacement can be compensated during the motion planning of the robot using the information from Fig. S.1ⓔ.

In a variation of the robot-gripper design, the Tail gripper is assembled onto the Millipede robot in an inverted configuration in order to facilitate grasping of objects from the substrate. In this experiment, the grasping function followed by locomotion of the robot is achieved successfully (Fig. 8ⓐ, Video SV4). However, it requires the target object to be beneath the Tail, and the robot cannot be maneuvered into position to pick up the object. Also, after grasping, the Tail drags the object on the substrate, which is deemed less preferable compared to the safe tethering of the object on top of the robot seen in the previous experiments. Alternatively, the Tail gripper can also be used to securely transport and release substances to target locations within the workspace (Fig. 8ⓑ, Video SV4). To demonstrate this, a color dye (Sudan Orange, Merck KGaA, Germany) is mixed into a water-soluble gel (Aquasonic 100, Parker Laboratories Inc., USA) and applied to a Tail gripper on a Millipede robot. The robot maneuvers to the target location and the dye-coated gel is applied onto the substrate by unwrapping the Tail gripper. After the substance is applied at the target site, the robot can navigate to other locations without staining any other part of the workspace. The Tail gripper can also hold onto cargo even after the actuating magnetic field is removed (Video SV4).

The experiments with the Hexapod robots and the Flower grippers are shown in Fig. 9. In the first experiment (Fig. 9ⓐ, Video SV5), the robot is able to navigate obstacles while turning either left or right, demonstrating that the maneuverability of the robot is not compromised when the gripper is attached to it. The second experiment (Fig. 9ⓑ, Video SV5) shows a pick-and-place procedure being performed by the robot where it moves forward with minimal activation of the gripper, opens the gripper to envelop an object (a ball of felt), and closes the gripper to grab the object. The Hexapod robot then holds on to the object, navigates to a second location within the workspace, and drops off the object in the target area by opening the gripper before moving away. This demonstrates the ability of the Hexapod robot and the Flower gripper to be activated selectively, with the gripper opening and closing only when picking up the object and again at the target site. Due to the closed shape of the Flower gripper, it can also retain cargo without the need for constant actuation.

4. Conclusions and future work

In this paper, two untethered magnetic soft robots with grasping manipulators capable of executing pick-and-place tasks are demonstrated. Novel designs for two multi-limbed soft robots and two grippers are developed, using inspiration from nature. The primary focus is on achieving tandem actuation of different functions (locomotion and grasping) on two separate elements within a single soft robot using torques generated through external magnetic fields. This has been achieved by engineering the actuation response of the robots and grippers such that decoupled actuation of either function is possible by varying the magnitude, frequency and orientation of the external magnetic field. Maneuverability during legged locomotion is achieved by biasing the actuation response of the legs such that displacement on either side of the robot can be varied to produce turning motion. The Millipede robot shows good repeatability and stable locomotion using the rhythmic magnetization pattern, and requires only a single control input to change its heading. The Hexapod robot moves using a alternating tripod gait, and requires a simpler fabrication process in comparison to the Millipede robot. The Tail gripper grasps by rolling around an object under a rotating magnetic field, while the Flower gripper is activated by a

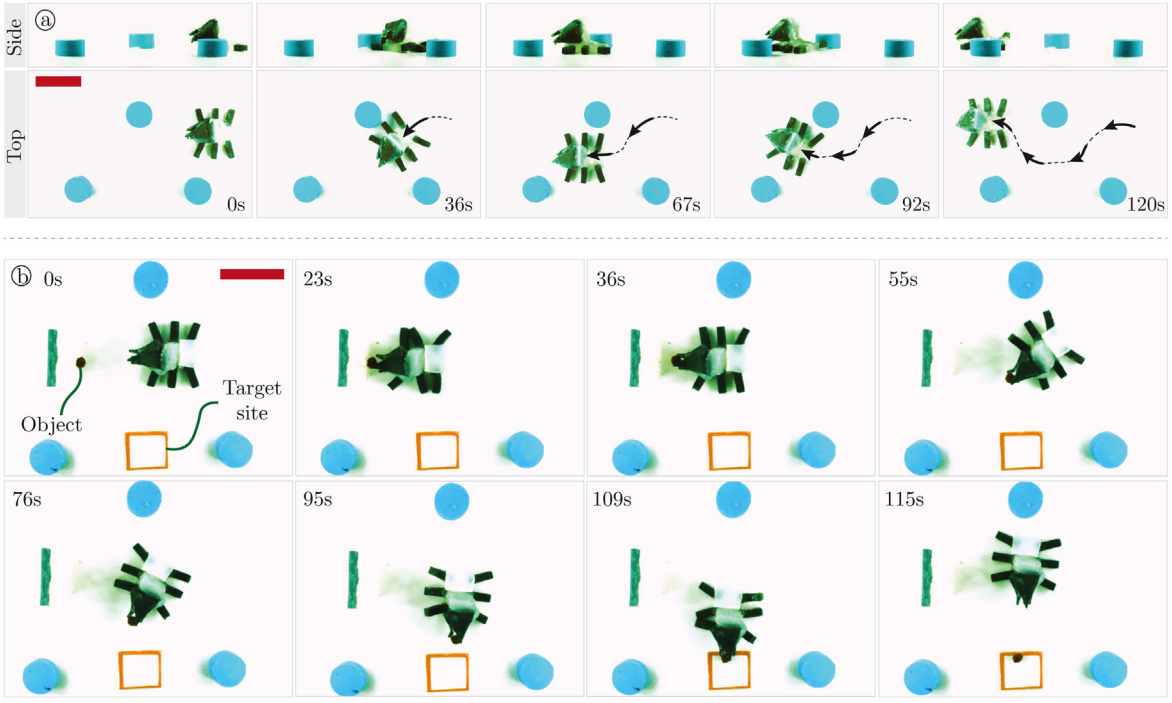

Fig. 9. ⓐ Experiment demonstrating Hexapod robot with Flower gripper navigating obstacles in the workspace. The locomotion of the robot is achieved using the actuation method described in Section 3.2, which ensures that the gripper is minimally affected (15 [mT] at 1 [Hz]). ⓑ Experiment demonstrating Hexapod robot with Flower gripper performing a pick-and-place procedure. The robot first moves towards the object (attached to green wall), grasps it by activating the gripper (30 [mT] at 1 [Hz]), then navigates to a target site without triggering the gripper, and deposits the object by actuating the gripper. Scale bar is 10 [mm]. (For interpretation of the references to color in this figure legend, the reader is referred to the web version of this article.)

magnetic field directed along its axis and opens and closes to hold an object inside. Neither gripper requires constant activation in order to hold cargo. Controllable steering is demonstrated through experiments where the robots navigate around obstacles under teleoperation. The combinations of the robots and the grippers are successfully tested to perform pick-and-place tasks by grasping and releasing objects when triggered using magnetic fields.

The legged locomotion of the robots provides advantages over grippers that move over substrates via rolling locomotion. As an example, if the robot is carrying a camera or an attached sensor for localization, legged locomotion would be preferable to rolling locomotion. In this paper, the use of legged locomotion to ensure secure transport of substances to target locations without exposing other parts of the workspace to said substance is also demonstrated. The grasping demonstrations shown in this paper are constrained by the positions of the grippers. However, this does not limit their use for transport and delivery of cargo to target locations. It would also be possible to adjust the positions of the grippers to suit certain applications (for instance, grasping from the substrate using the Tail gripper is demonstrated).

The robots presented in this work are intended for potential applications such as inspection of constrained or enclosed spaces and acquiring target objects in scenarios where a mechanical tether would be infeasible. One particular area of interest is minimally invasive surgical interventions, where these types of robots can be used for targeted therapeutic applications, such as diagnostic imaging, biopsy or drug delivery. In particular, the robots described in this paper would be suitable for procedures in the gastrointestinal tract, where the organs are sufficiently large to allow the use of centimeter-scale robots. Also, these organs are usually emptied before surgery, enabling the robots to move across the surface of the organs where legged locomotion could have potential benefits when compared to dragging motion using magnetic forces. However, miniaturization of the robots could still be useful, with developments in materials and manufacturing opening up the possibility of producing these robots at different dimension scales, including sub millimeter sizes. It is worth mentioning that the actuation of the robots also needs to be improved in other aspects (such as motion on non-horizontal surfaces, remote tracking and control) before they can be used for real-world application.

In this work, the actuation response of the functional elements (i.e. the orientations of magnetic dipoles) is hard coded into their structure, which necessitates careful design and actuation. For instance, it would not be possible to combine the Hexapod robot with the Tail gripper. In order to achieve increased variability in function, it is necessary to develop actively-reconfigurable magnetic elements, perhaps using miniaturized electromagnetic coils.

The teleoperated experiments demonstrate the potential for autonomous operation of the soft robots and grippers. Adding sensory elements and localization capabilities is necessary in application-relevant scenarios. The central bodies of both robots presented here are non-magnetic and require minimal flexibility, suggesting the possibility of replacing the silicone with other functional components. The use of other smart materials within the magnetic polymer composite and developments in the design of electromagnetic actuation systems would also open up the range of applications for these types of soft robots.

Declaration of competing interest

The authors declare that they have no known competing financial interests or personal relationships that could have appeared to influence the work reported in this paper.

Acknowledgments

This research has received funding from the European Research Council (ERC) under the European Union's Horizon 2020 Research and Innovation programme (Grant Agreement #638428 — project ROBOTAR). The authors would like to thank Leon Abelmann and Yannick Klein for their help with magnetization of samples.

Appendix A. Supplementary data

Supplementary material related to this article can be found online at https://doi.org/10.1016/j.eml.2020.101023.

References

[1] R. Pfeifer, M. Lungarella, F. Iida, Self-organization, embodiment, and biologically inspired robotics, Science 318 (5853) (2007) 1088–1093.
[2] D. Rus, M.T. Tolley, Design, fabrication and control of soft robots, Nature 521 (7553) (2015) 467–475.
[3] C. Majidi, Soft robotics: A perspective—Current trends and prospects for the future, Soft Robot. 1 (1) (2013) 5–11.
[4] M.T. Tolley, R.F. Shepherd, B. Mosadegh, K.C. Galloway, M. Wehner, M. Karpelson, R.J. Wood, G.M. Whitesides, A resilient, untethered soft robot, Soft Robot. 1 (3) (2014) 213–223.
[5] C. Laschi, M. Cianchetti, B. Mazzolai, L. Margheri, M. Follador, P. Dario, Soft robot Arm inspired by the octopus, Adv. Robot. 26 (7) (2012) 709–727.
[6] S. Kim, C. Laschi, B. Trimmer, Soft robotics: a bioinspired evolution in robotics, Trends Biotechnol. 31 (5) (2013) 287–294.
[7] K.-J. Cho, R. Wood, Biomimetic robots, in: B. Siciliano, O. Khatib (Eds.), Springer Handbook of Robotics, Springer International Publishing, Cham, 2016, pp. 543–574.
[8] M. Wehner, R.L. Truby, D.J. Fitzgerald, B. Mosadegh, G.M. Whitesides, J.A. Lewis, R.J. Wood, An integrated design and fabrication strategy for entirely soft, autonomous robots, Nature 536 (7617) (2016) 451–455.
[9] E.T. Roche, R. Wohlfarth, J.T.B. Overvelde, N.V. Vasilyev, F.A. Pigula, D.J. Mooney, K. Bertoldi, C.J. Walsh, A bioinspired soft actuated material, Adv. Mater. 26 (8) (2014) 1200–1206.
[10] E.B. Dolan, C.E. Varela, K. Mendez, W. Whyte, R.E. Levey, S.T. Robinson, E. Maye, J. O'Dwyer, R. Beatty, A. Rothman, Y. Fan, J. Hochstein, S.E. Rothenbucher, R. Wylie, J.R. Starr, M. Monaghan, P. Dockery, G.P. Duffy, E.T. Roche, An actuatable soft reservoir modulates host foreign body response, Sci. Robot. 4 (33) (2019) eaax7043.
[11] M. Runciman, A. Darzi, G.P. Mylonas, Soft robotics in minimally invasive surgery, Soft Robot. 6 (4) (2019) 423–443.
[12] J. Cui, T.-Y. Huang, Z. Luo, P. Testa, H. Gu, X.-Z. Chen, B.J. Nelson, L.J. Heyderman, Nanomagnetic encoding of shape-morphing micromachines, Nature 575 (7781) (2019) 164–168.
[13] M. Sitti, H. Ceylan, W. Hu, J. Giltinan, M. Turan, S. Yim, E. Diller, Biomedical applications of untethered mobile milli/microrobots, Proc. IEEE 103 (2) (2015) 205–224.
[14] B.J. Nelson, I.K. Kaliakatsos, J.J. Abbott, Microrobots for minimally invasive medicine, Annu. Rev. Biomed. Eng. 12 (1) (2010) 55–85.
[15] J. Kim, S.E. Chung, S.-E. Choi, H. Lee, J. Kim, S. Kwon, Programming magnetic anisotropy in polymeric microactuators, Nature Mater. 10 (10) (2011) nmat3090.
[16] G.Z. Lum, Z. Ye, X. Dong, H. Marvi, O. Erin, W. Hu, M. Sitti, Shape-programmable magnetic soft matter, Proc. Natl. Acad. Sci. 113 (41) (2016) E6007–E6015.
[17] V.Q. Nguyen, A.S. Ahmed, R.V. Ramanujan, Morphing soft magnetic composites, Adv. Mater. 24 (30) (2012) 4041–4054.
[18] Y. Kim, G.A. Parada, S. Liu, X. Zhao, Ferromagnetic soft continuum robots, Sci. Robot. 4 (33) (2019) eaax7329.
[19] P. Garstecki, P. Tierno, D.B. Weibel, F. Sagues, G.M. Whitesides, Propulsion of flexible polymer structures in a rotating magnetic field, J. Phys.: Condens. Matter 21 (20) (2009).
[20] W. Hu, G.Z. Lum, M. Mastrangeli, M. Sitti, Small-scale soft-bodied robot with multimodal locomotion, Nature 554 (7690) (2018) 81–85.
[21] J. Zhang, E. Diller, Untethered miniature soft robots: Modeling and design of a Millimeter-scale swimming magnetic sheet, Soft Robot. 5 (6) (2018) 761–776.
[22] J.B. Mathieu, S. Martel, L. Yahia, G. Soulez, G. Beaudoin, Preliminary studies for using magnetic resonance imaging systems as a mean of propulsion for microrobots in blood vessels and evaluation of ferromagnetic artefacts, in: CCECE 2003 - Canadian Conference on Electrical and Computer Engineering. Toward a Caring and Humane Technology (Cat. No.03CH37436), Vol. 2, 2003, pp. 835–838.
[23] S. Jeon, A.K. Hoshiar, K. Kim, S. Lee, E. Kim, S. Lee, J.-y. Kim, B.J. Nelson, H.-J. Cha, B.-J. Yi, H. Choi, A magnetically controlled soft Microrobot steering a Guidewire in a three-dimensional Phantom vascular network, Soft Robot. 6 (1) (2018).
[24] A. Azizi, C.C. Tremblay, K. Gagné, S. Martel, Using the fringe field of a clinical MRI scanner enables robotic navigation of tethered instruments in deeper vascular regions, Sci. Robot. 4 (36) (2019) eaax7342.
[25] Y. Kim, H. Yuk, R. Zhao, S.A. Chester, X. Zhao, Printing ferromagnetic domains for untethered fast-transforming soft materials, Nature 558 (7709) (2018) 274–279.
[26] H. Lu, M. Zhang, Y. Yang, Q. Huang, T. Fukuda, Z. Wang, Y. Shen, A bioinspired multilegged soft millirobot that functions in both dry and wet conditions, Nature Commun. 9 (1) (2018) 3944.
[27] T. Xu, J. Zhang, M. Salehizadeh, O. Onaizah, E. Diller, Millimeter-scale flexible robots with programmable three-dimensional magnetization and motions, Sci. Robot. 4 (29) (2019) eaav4494.
[28] C. Pacchierotti, F. Ongaro, F. van den Brink, C. Yoon, D. Prattichizzo, D.H. Gracias, S. Misra, Steering and control of miniaturized untethered soft magnetic grippers with haptic assistance, IEEE Trans. Autom. Sci. Eng. 15 (1) (2018) 290–306.
[29] A. Ghosh, C. Yoon, F. Ongaro, S. Scheggi, F.M. Selaru, S. Misra, D.H. Gracias, Stimuli-responsive soft untethered grippers for drug delivery and robotic surgery, Front. Mech. Eng. 3 (2017).
[30] S. Fusco, M.S. Sakar, S. Kennedy, C. Peters, S. Pane, D. Mooney, B.J. Nelson, Self-folding mobile microrobots for biomedical applications, in: 2014 IEEE International Conference on Robotics and Automation (ICRA), 2014, pp. 3777–3782, ISSN: 1050-4729.
[31] E. Diller, M. Sitti, Three-dimensional programmable assembly by untethered magnetic robotic Micro-Grippers, Adv. Funct. Mater. 24 (28) (2014) 4397–4404.
[32] M.P.d. Cunha, Y. Foelen, R.J.H.v. Raak, J.N. Murphy, T.A.P. Engels, M.G. Debije, A.P.H.J. Schenning, An untethered magnetic- and light-responsive rotary gripper: Shedding light on photoresponsive liquid crystal actuators, Adv. Opt. Mater. 7 (7) (2019) 1801643.
[33] S.E. Chung, X. Dong, M. Sitti, Three-dimensional heterogeneous assembly of coded microgels using an untethered mobile microgripper, Lab Chip 15 (7) (2015) 1667–1676.
[34] J. Zhang, O. Onaizah, K. Middleton, L. You, E. Diller, Reliable grasping of three-dimensional untethered mobile magnetic microgripper for autonomous pick-and-place, IEEE Robot. Autom. Lett. 2 (2) (2017) 835–840.
[35] J. Sikorski, I. Dawson, A. Denasi, E.E.G. Hekman, S. Misra, Introducing BigMag - a novel system for 3D magnetic actuation of flexible surgical manipulators, in: 2017 IEEE International Conference on Robotics and Automation (ICRA), 2017, pp. 3594–3599.
[36] M. Golubitsky, I. Stewart, P.-L. Buono, J.J. Collins, Symmetry in locomotor central pattern generators and animal gaits, Nature 401 (6754) (1999) 693–695.
[37] A. Torige, M. Noguchi, N. Ishizawa, Centipede type multi-legged walking robot, in: Proceedings of 1993 IEEE/RSJ International Conference on Intelligent Robots and Systems (IROS '93), Vol. 1, 1993, pp. 567–571.
[38] K.L. Hoffman, R.J. Wood, Myriapod-like ambulation of a segmented microrobot, Auton. Robots 31 (1) (2011) 103.
[39] V.K. Venkiteswaran, L.F.P. Samaniego, J. Sikorski, S. Misra, Bio-inspired Terrestrial motion of magnetic soft Millirobots, IEEE Robot. Autom. Lett. 4 (2) (2019) 1753–1759.
[40] T. Lee, C. Liao, T.K. Chen, On the stability properties of hexapod tripod gait, IEEE J. Robot. Autom. 4 (4) (1988) 427–434.
[41] P. Birkmeyer, K. Peterson, R.S. Fearing, DASH: A dynamic 16g hexapedal robot, in: 2009 IEEE/RSJ International Conference on Intelligent Robots and Systems, 2009, pp. 2683–2689.